XIV International Conference on Computational Plasticity. Fundamentals and Applications
COMPLAS XIV
E. Oñate, D.R.J. Owen, D. Peric & M. Chiumenti (Eds)

THE PERFORMANCE AND PREDICTION ABILITY OF ADVANCED APPROACH TO DUCTILE FRACTURE

FRANTIŠEK ŠEBEK, JINDŘICH PETRUŠKA* AND PETR KUBÍK

* Faculty of Mechanical Engineering
Brno University of Technology
Technická 2896/2, 616 69 Brno, Czech Republic
e-mail: petruska@fme.vutbr.cz, web page: http://www.fme.vutbr.cz/

Key words: Rupture, Failure, Weakening, Coupled damage, Continuum Damage Mechanics

Abstract. The present paper deals with the modelling of ductile fracture which is the result of severe plastic deformation under monotonic loading. It can be the result of a crash or accident or introduced intentionally. There is a need of increasing the safety in many fields of industrial sector or transportation. The aluminium alloy 2024-T351 is widely used for studies of ductile fracture. The material was supplied as a cold-rolled plate for this study and examined within a broad range of stress states. First of all, the flow curve was determined using the standard tensile test of smooth cylindrical bar. Then, the tensile tests of variously notched cylindrical bars were conducted to show the pressure dependence. The tensile and torsion tests of notched tube were added in order to document the dependency on the deviatoric stress state. Finally, the compression test of smooth cylinder was executed. Then, deviatoric stress state dependent plasticity and the original ductile fracture hyperbolic criterion were calibrated. The damage accumulation nonlinearity was examined through loading–unloading experiments. The double damage curve approach, inspired by the fatigue life prediction, was revisited and calibrated using the semi-cyclic testing. Finally, the softening effect was studied aiming to couple the damage with plasticity. The performance and prediction ability was verified after the model was completely calibrated and implemented into the Abaqus finite element software. Three different cases of tension were chosen for this comparative purpose. The tension of notched cylindrical and tubular specimens and flat specimen. The ductile fracture criterion coupled with plasticity should provide the slant fracture in the conditions of plane strain due to localization. Nevertheless, it is shown that the proposed approach has still some drawbacks in prediction of the crack propagation.

1 INTRODUCTION

The ductile fracture has been studied using different approaches and for various applications so far [1, 2, 3].

One measure can be the ability to produce a similar mode of cracking [4] and the other perceives the global performance [5, 6]. The ability to describe the plastic behaviour remains one of the cornerstones when concerning the uncoupled ductile fracture criteria [7, 8]. Notwithstanding how well the phenomenological criterion is calibrated, it is crucial what history preceded the crack initiation [9]. Then, there is a transition in the form of partially coupled criteria which brings the important advantage in more realistic crack propagation [10]. Besides the ability to produce the slant fracture, the coupled ductile fracture criteria provide a tool how to put the plasticity and damage together. Apart from the criteria based on Gurson-type model [11], which incorporates the damage directly into the plasticity, the plasticity and damage are computed along each other and influence one another [12]. Then, various possibilities are opened for describing the material behaviour which can be useful in vast area of applications [13, 14, 15].

The purpose of this paper is to design a set of reliable fracture tests and to develop a universal ductile fracture criterion. Aluminium alloy 2024-T351 was chosen for those studies as a suitable candidate [16]. It has been widely used in aerospace industry [17]. The plasticity is another feature of the whole model. It was considered as a non-quadratic one to describe different behaviour at uniaxial tension and plane strain. It is suitable to couple the plasticity with damage to make the approach advanced as much as possible. This can be realized through weakening. The nonlinear damage accumulation is the last important part of the approach. It was shown that it is not suitable to investigate it through the step-wise testing [18], but rather using loading–unloading experiments [8]. The verification of results were conducted on three cases of tension. Tension of notched cylindrical and tubular specimens, covered in calibration and describing the tensile axial symmetry and plane strain tension, and additional test – tension of flat plate.

2 YIELD CRITERION

First of all, the tensile test of smooth cylindrical specimen was conducted. Then, the flow curve was estimated (Fig. 1a). It is very useful to use the approach of Xue [19] who introduced the flow curve of matrix. In our case, this curve (Fig. 1b) was obtained by multiplying the flow stress by correction function ($m = 1$ during plasticity calibration)

$$m = 1 + \bar{\epsilon}^p, \tag{1}$$

where $\bar{\epsilon}^p$ is the equivalent plastic strain. It was revealed that the behaviour of studied aluminium alloy cannot be described by quadratic von Mises plasticity well [20]. Instead, the yield criterion proposed by Kroon and Faleskog [21] was adopted. Yield function is

$$\Phi = \bar{\sigma} - m w \sigma_Y k, \tag{2}$$

where $\bar{\sigma}$ is the equivalent von Mises stress, w is the weakening function ($w = 1$ during plasticity calibration), σ_Y is the yield stress, and k is the yield function correction as

$$k = 1 - \gamma\omega \left(\frac{1 + \omega_0^{\frac{1}{a}}}{\omega^{\frac{1}{a}} + \omega_0^{\frac{1}{a}}} \right)^a, \tag{3}$$

where $\gamma = 0.123$, $\omega_0 = 0.18$ and $a = 4$ are calibrated material constants, so it is close to Tresca yield criterion, and ω is the normalized Lode parameter [22].

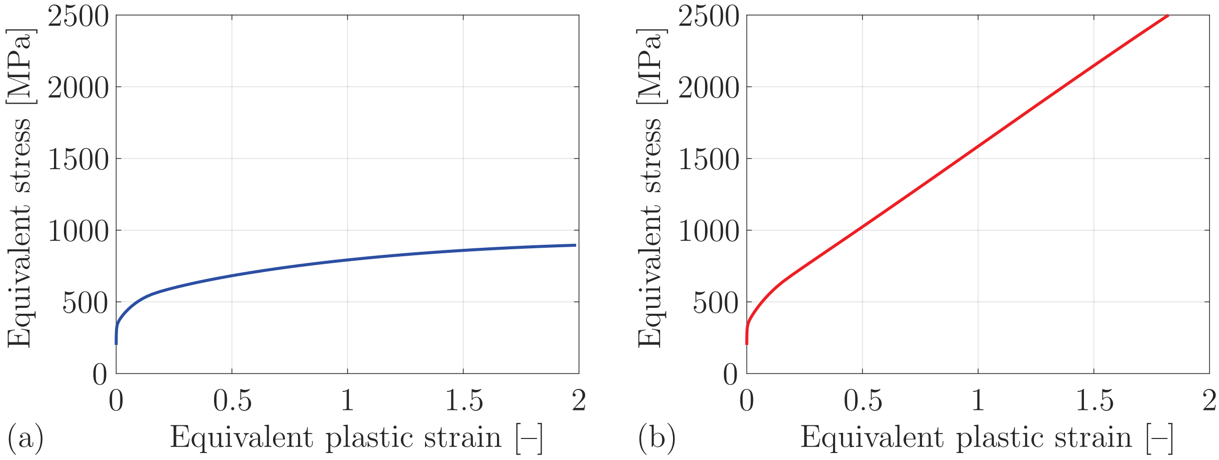

Figure 1: The flow curve: (a) conventional; (b) of matrix material

3 DAMAGE ACCUMULATION

The semi-cyclic testing was used to study the nonlinear damage accumulation. First, the damage parameter can be estimated as [23]

$$D = 1 - \frac{\bar{E}}{E}, \tag{4}$$

where $\bar{E}$ is the actual degraded Young's modulus and E is the virgin Young's modulus.

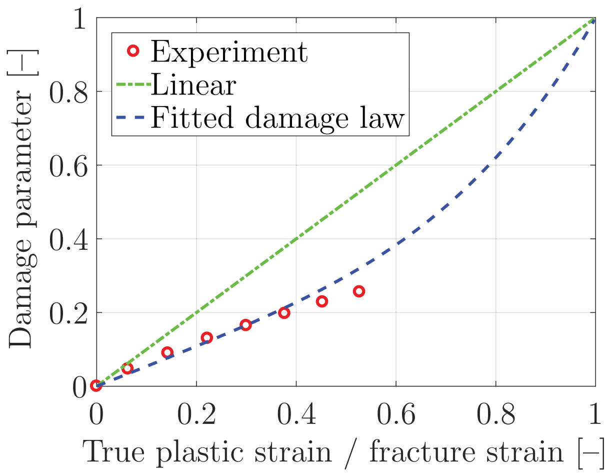

Figure 2: The semi-cyclic testing and fitted nonlinear damage accumulation

Then, the double damage curve approach proposed by Manson and Halford [24] for fatigue was revisited. The damage parameter reads

$$D = \int_0^{\hat{\epsilon}^D} q_1 \frac{d\bar{\epsilon}^p}{C + \bar{\epsilon}^f} + \int_0^{\hat{\epsilon}^D} q_2(1 - q_1) \left(\frac{\bar{\epsilon}^p}{C + \bar{\epsilon}^f} \right) \frac{d\bar{\epsilon}^p}{C + \bar{\epsilon}^f}, \tag{5}$$

where $\hat{\epsilon}^D$ is the equivalent plastic strain for a given loading path, q_1, q_2 and C are three material constants and $\bar{\epsilon}^f$ is the fracture envelope.

The two material constants were calibrated using the semi-cyclic experiments (Fig. 2) as $q_1 = 0.54$ and $q_2 = 4$.

4 MATERIAL WEAKENING

The material weakening is realized through the weakening function mentioned earlier

$$w = 1 - D^{\beta}, \tag{6}$$

where β is the weakening exponent. It was calibrated together with constant C to fit the tensile test of smooth cylindrical specimen (Fig. 3) as $\beta = 1.1$ and $C = 0.28$.

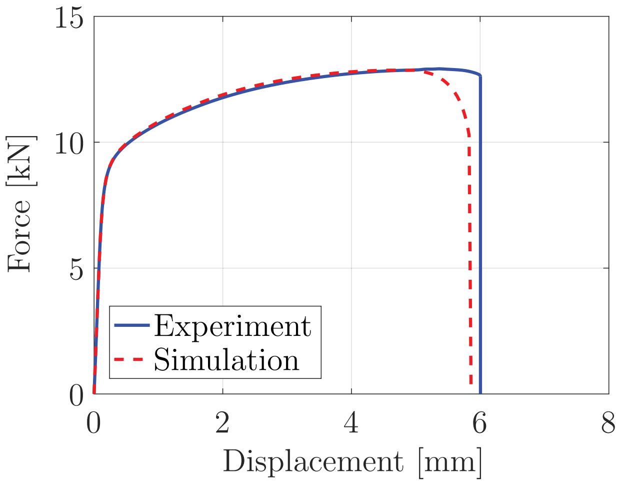

Figure 3: The force–displacement response for calibrated constants β and C

5 DUCTILE FRACTURE CRITERION

Table 1: Calibrated material constants for 2024-T351

G_1	G_2	G_3	G_4	G_5	G_6
−0.178	1.195	1.189	0.104	0.301	0.327

The hyperbolic ductile fracture criterion KHPS2 was proposed. It is based on KHPS criterion [25]. It has the fracture envelope as

$$\bar{\epsilon}^f = \left[\frac{1}{2}\left(\frac{G_4}{\langle \eta + g\rangle} + \frac{G_5}{\langle \eta + g\rangle}\right) - \frac{G_6}{\langle \eta + g\rangle}\right]\xi^2 + \frac{1}{2}\left(\frac{G_4}{\langle \eta + g\rangle} + \frac{G_5}{\langle \eta + g\rangle}\right)\xi + \frac{G_6}{\langle \eta + g\rangle}, \tag{7}$$

where $G_1, \ldots, G_6$ are material constants given in Tab. 1, ξ is the normalized third invariant of the deviatoric stress tensor, η is the stress triaxiality and g is the parabolic cut-off

$$g = \left(G_3 + \frac{G_1 - G_3}{2} - G_2\right)\xi^2 + \frac{G_1 - G_3}{2}\xi + G_2. \tag{8}$$

6 PREDICTION SIMULATIONS

There were chosen three different cases for examination of the performance and prediction ability under tension.

The first is the tension of notched cylindrical specimen. The force–displacement response is predicted slightly higher with also higher displacement at fracture (Fig. 4). The proposed approach predicted the slant fracture in the final stage of cracking, similarly as in the experiment (Fig. 4). Nevertheless, the classical cup and cone fracture was not observed experimentally.

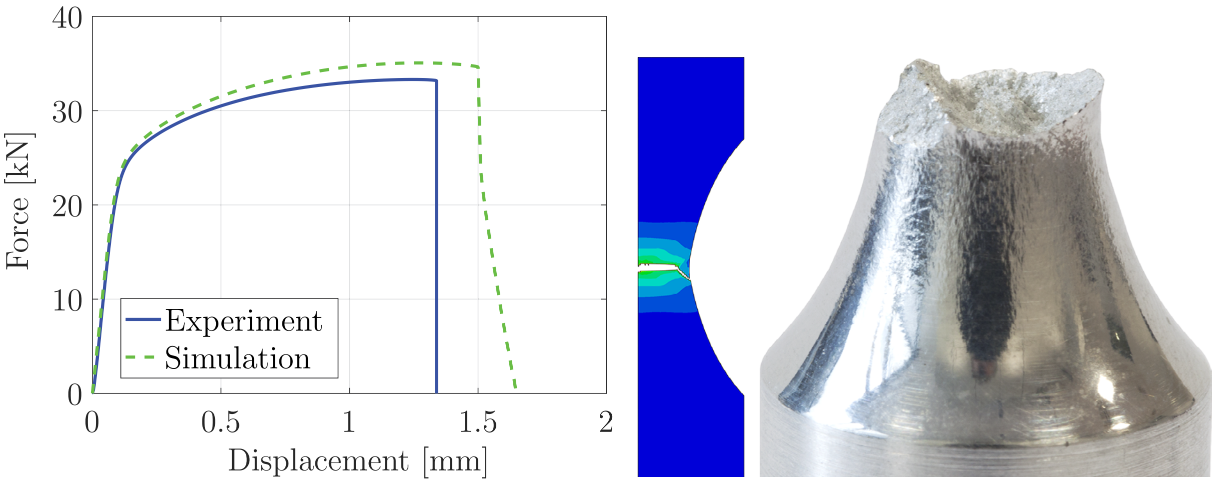

Figure 4: The responses for notched cylindrical specimen and specimens from experiment and simulation

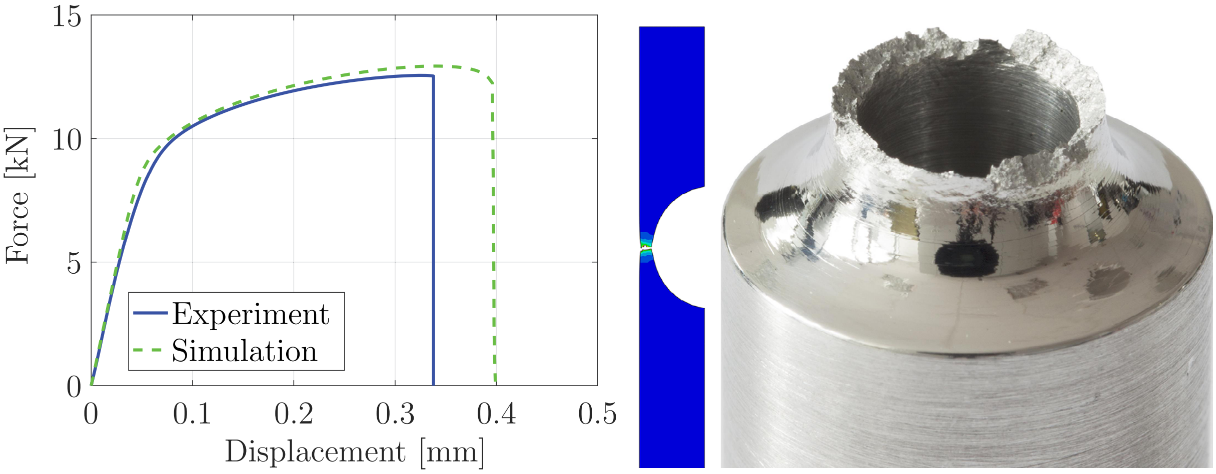

Figure 5: The responses for notched tubular specimen and specimens from experiment and simulation

The second case is the tension of notched tubular specimen. The shape of force–displacement curve is captured very well but the model still predicted higher displacement at fracture (Fig. 5). The slant fracture was not predicted by the model as in the experiment (Fig. 5).

The last simulation is the tension of flat plate. The material behaviour at plane strain or generalized shear was described well the by non-quadratic yield criterion. The material often obeys lower ductility at this region in comparison to uniaxial tension, as tested at previous case. The displacement at fracture is grossly over predicted. On the other hand, the typical slant fracture was formed the same as experimentally observed (Fig. 6).

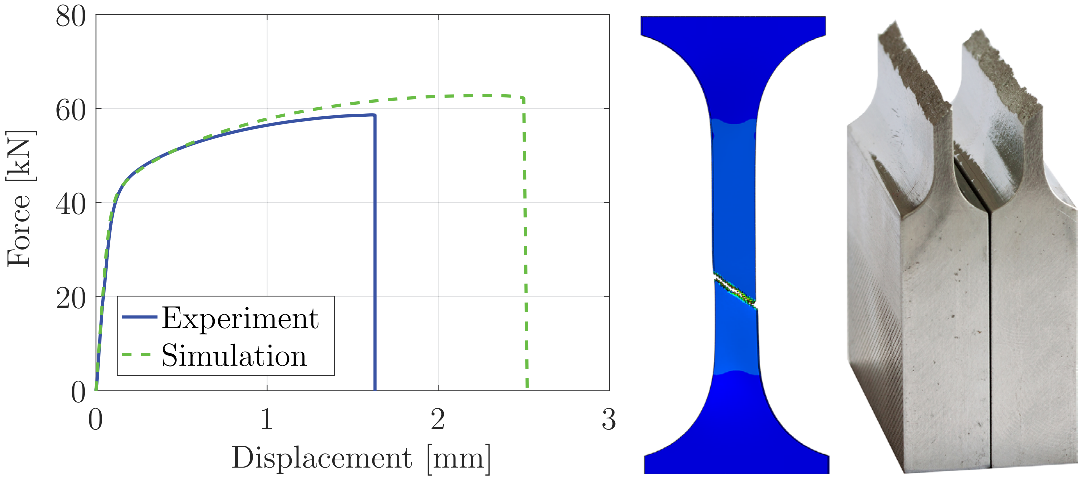

Figure 6: The responses for flat plate specimen and specimens from experiment and simulation

The results suggest that the constant C should be lower, so it would prevent the late cracking. On the other hand, it would deteriorate the force–displacement response of smooth cylindrical specimen (Fig. 3), where the early cracking would occur.

7 CONCLUSIONS

The present paper dealt with ductile fracture. Proposed criterion KHPS2 was calibrated using tensile smooth and notched cylindrical specimens, tensile and torsional notched tube specimens and upsetting cylinder. The damage was coupled with plasticity to form the coupled model in the sense of continuum damage mechanics.

The model was verified under the tensile loading. The force–displacement curves were described well in overall, but there were some drawbacks in over estimating the final fracture. The remarkable difference was observed at plane strain tension. This discrepancy could be attributed to the different stress state. It is expected that the normalized third invariant of deviatoric stress tensor should be zero but it tends to approach unity [21, 26]. Nevertheless, this should also affect the flow behaviour which still seems to be described well contrary to that.

The fracture surfaces were predicted in correspondence with experimental observation, except for the tension of notched tubular specimen. This could by caused by a very small thickness of the specimen wall.

The model should be examined further. It would be also useful to conduct more extensive experimental program and test the aluminium alloy 2024-T351 under more stress states.

8 ACKNOWLEDGEMENT

This work is an output of project NETME CENTRE PLUS (LO1202) created with financial support from the Ministry of Education, Youth and Sports under the "National Sustainability Programme I".

REFERENCES

[1] Dunand, M. and Mohr, D. On the predictive capabilities of the shear modified Gurson and the modified Mohr–Coulomb fracture models over a wide range of stress triaxialities and Lode angles. *J. Mech. Phys. Solids* (2011) **59**:1374–1394.

[2] Törnqvist, R. *Design of crashworthy ship structures*. PhD Thesis, Technical University of Denmark (2003).

[3] Komori, K. Simulation of crack arrest in blanking using the node separation method. *Int. J. Mech. Sci.* (2013) **68**:150–159.

[4] Kubík, P., Šebek, F. and Petruška, J. Ductile fracture criteria in prediction of slant fracture. In *ECCOMAS Congress 2016*, 6699–6710 (2016).

[5] Pack, K., Luo, M. and Wierzbicki, T. Sandia fracture challenge: Blind prediction and full calibration to enhance fracture predictability. *Int. J. Fract.* (2014) **186**:155–175.

[6] Papasidero, J., Doquet, V. and Mohr, D. Ductile fracture of aluminum 2024-T351 under proportional and non-proportional multi-axial loading: Bao–Wierzbicki results revisited. *Int. J. Solids Struct.* (2015) **69–70**:459–474.

[7] Joun, MS., Eom, J.G. and Lee, M.Ch. A new method for acquiring true stress–strain curves over a large range of strains using a tensile test and finite element method. *Mech. Mater.* (2008) **40**:586–593.

[8] Celentano, D.J. and Chaboche, J.-L. Experimental and numerical characterization of damage evolution in steels. *Int. J. Plast.* (2007) **23**:1739–1762.

[9] Beese, A.M., Luo, M., Li, Y., Bai, Y. and Wierzbicki, T. Partially coupled anisotropic fracture model for aluminum sheets. *Eng. Fract. Mech.* (2010) **77**:1128–1152.

[10] Šebek, F., Kubík, P. and Petruška, J. Localization problem of coupled ductile failure models compared to uncoupled ones. In *Engineering Mechanics 2014*, 632–635 (2014).

[11] Türtük, İ.C. and Deliktaş, B. Coupled porous plasticity – Continuum damage mechanics approaches for modelling temperature driven ductile-to-brittle transition fracture in ferritic steels. *Int. J. Plast.* (2016) **77**:246–261.

[12] Šebek, F., Hůlka, J., Kubík, P. and Petruška, J. On the proportionality of damage rule in finite element simulations of the ductile failure. *Adv. Mater. Res.* (2014) **980**:189–193.

[13] Petruška, J., Návrat, T. and Šebek, F. A new model for fast analysis of leveling process. *Adv. Mater. Res.* (2012) **586**:389–393.

[14] Petruška, J., Návrat, T., Šebek, F. and Benešovský, M. Optimal intermeshing of multi roller cross roll straightening machine. *AIP Conf. Proc.* (2016) **1769**:120002-1–120002-4.

[15] Peč, M., Kubík, P., Šebek, F., Návrat, T. and Petruška, J. Modeling of the blast load effects in explicit dynamics. In *Engineering Mechanics 2016*, 442–445 (2016).

[16] Papasidero, J., Doquet, V. and Lepeer, S. Multiscale investigation of ductile fracture mechanisms and strain localization under shear loading in 2024-T351 aluminum alloy and 36NiCrMo16 steel. *Mater. Sci. Eng. A* (2014) **610**:203–219.

[17] Rodríguez-Millán, M., Vaz-Romero, Á and Arias, Á. Failure behavior of 2024-T3 aluminum under tension-torsion conditions. *J. Mech. Sci. Technol.* (2015) **29**:4657–4663.

[18] Šebek, F., Petruška, J. and Kubík, P. The role of loading path in ductile fracture. In *6th International Conference on Structural Engineering, Mechanics and Computation 2016*, 550–555 (2016).

[19] Xue, L. *Ductile fracture modeling - Theory , experimental investigation and numerical verification.* PhD Thesis, Massachusetts Institute of Technology (2007).

[20] Peč, M., Vosynek, P., Šebek, F. and Návrat, T. Implementation of American weld connection standards into finite element computations. *IOP Conf. Ser.: Mater. Sci. Eng.* (2017) **179**:012056-1–012056-7.

[21] Kroon, M. and Faleskog, J. Numerical implementation of a J_2- and J_3-dependent plasticity model based on a spectral decomposition of the stress deviator. *Comput. Mech.* (2013) **52**:1059–1070.

[22] Nahshon, K. and Hutchinson J.W. Modification of the Gurson Model for shear failure. *Eur. J. Mech. A Solids* (2008) **27**:1–17.

[23] Lemaitre, J. Coupled elasto-plasticity and damage constitutive equations. *Comput. Methods Appl. Mech. Engrg.* (1985) **51**:31–49.

[24] Manson, S.S. and Halford, G.R. *Re-examination of cumulative fatigue damage analysis—An engineering perspective.* NASA Technical Memorandum 87325 (1985).

[25] Kubík, P., Šebek, F., Hůlka, J. and Petruška, J. Calibration of ductile fracture criteria at negative stress triaxiality. *Int. J. Mech .Sci.* (2016) **108–109**:90–103.

[26] Šebek, F., Petruška, J. and Kubík, P. Behavior of lode dependent plasticity at plane strain condition and its implication to ductile fracture. *Solid State Phenom.* (2017) **258**:213–216.